Solubility of the Single Gases Methane and Xenon in the Ionic Liquid [bmim][CH_3SO_4]

Jacek Kumełan, Álvaro Pérez-Salado Kamps, Dirk Tuma, and Gerd Maurer*

Chair of Applied Thermodynamics, University of Kaiserslautern, P. O. Box 30 49, D-67653 Kaiserslautern, Germany

Solubility measurements of methane and of xenon in the ionic liquid 1-*n*-butyl-3-methylimidazolium methyl sulfate ([bmim][CH_3SO_4]) were performed with a high-pressure view-cell technique based on the synthetic method. The temperature ranged from 293.1 K to 413.2 K, and the maximum pressure (the maximum gas molality) was 8.9 MPa (0.19 mol·kg^{-1}) for methane and 11.3 MPa (0.65 mol·kg^{-1}) for xenon. Both gases become less soluble in [bmim][CH_3SO_4] with rising temperature, but xenon shows a significantly higher solubility at all conditions investigated. An extension of Henry's law is employed to correlate the solubility pressures in both cases. The final results for the Henry's constant (at zero pressure) of methane and xenon in [bmim][CH_3SO_4] (on the molality scale) are correlated within the experimental uncertainty (about ± 1.3 %) by $\ln(k^{(0)}_{H,CH_4}/\text{MPa}) = 6.216 - 564.5/(T/\text{K}) - 0.002566(T/\text{K})$ and $\ln(k^{(0)}_{H,Xe}/\text{MPa}) = 5.5906 - 928/(T/\text{K}) - 0.00141(T/\text{K})$, respectively.

Introduction

This work continues a series of investigations on the solubility of single gases in the ionic liquid 1-*n*-butyl-3-methylimidazolium methyl sulfate ([bmim][CH_3SO_4]). Prior to this study, the solubility of carbon dioxide[1] as well as hydrogen and carbon monoxide[2] was investigated. Here, we present new experimental data for the solubility of methane and xenon in the ionic liquid mentioned above that were measured as solubility isotherms at temperatures from 293.1 K to 413.2 K in intervals of 40 K using a high-pressure view cell. The maximum pressure (the maximum gas molality) amounts to 8.9 MPa (0.19 mol·kg^{-1}) for methane and 11.3 MPa (0.65 mol·kg^{-1}) for xenon. The corresponding Henry's constant of methane and xenon was determined in the same way as described in our preceding papers.[1,2]

The existence of data for the solubility of methane in the ionic liquids [bmim][PF_6] and [bmim][BF_4] at elevated pressures published by Anthony et al.[3,4] (from Brennecke's group) is known to us, but no investigations (in any ionic liquid) employing xenon could be tracked so far.

Our motivation for measuring xenon solubility in an ionic liquid was induced by a research question from medicine. Xenon is the only noble gas to exhibit significant anesthetic potency, and compared with other anesthetic agents xenon exhibits several favorable characteristics for medical application.[5−9] The anesthetic effect of xenon is 1.5 times higher than that of nitrous oxide (N_2O), and the low blood-gas partition coefficient of 0.115 (mL gas/mL liquid at 37 °C, taken from Lynch III et al.)[5] enables rapid inflow and washout during the application regardless of the duration of anesthesia. For nitrous oxide, medical literature reports the values of 0.46[6] and 0.47.[7] Consequently, the risk of diffusion hypoxia is less compared to more highly soluble anesthetic agents. Another important argument in favor of xenon is the reduced workplace and environmental hazards compared to traditional inhalation agents. Xenon should not affect the ozone layer, as do nitrous oxide and chlorine containing fluorocarbons. Unfortunately, xenon is very rare on earth. The atmosphere contains xenon in a concentration not more than 0.086 ppm. To illustrate this figure, a room with a volume of 100 m^3 contains approximately 8 mL xenon.[5] Therefore, xenon anesthesia will be costly, and the employment of this gas in anesthesia can be economically justified only if its waste is reduced to the minimum. According to Goto et al.,[8] to anesthetize a 70 kg adult human being with minimum alveolar concentration of xenon (71 %, cf. Lynch III et al.)[5] for 240 min 16 L (at 293.15 K and 0.101325 MPa) is consumed if xenon is applied via a closed rebreathing system. To obtain xenon from air during fractional distillation of liquefied air involves multiple energy-consuming heating, cooling, and pressurization processes. Because the waste anesthetic gas usually contains much higher concentrations of xenon (e.g., 50 % to 60 %),[8] its retrieval should be easier. For this purpose, prototypes were constructed that operate a liquefaction process of a 70 % xenon mixture at −20 °C but at a pressure of > 60 bar. Xenon gas is liquefied and can be stored for reuse or dispatch, whereas oxygen and nitrogen remain gaseous. The most efficient devices already reach a recycling rate of more than 90 % with 99 % gas purity.[6] However, any recycling concept that is based on liquefaction is hardly suitable for practical clinical use, mostly because of its size and operational demand. An alternative concept might be based on the use of ionic liquids. Actually, as found in our experiments, the ionic liquid [bmim][CH_3SO_4] is a remarkably good solvent for xenon and can already absorb considerable quantities under relatively mild conditions.

Experimental Section and Results

Apparatus and Method. We employed the same apparatus and the corresponding measuring technique as reported previously.[1,2] For a detailed outline, the reader is referred to these publications[1,2] and the references cited therein.

The mass of the gas introduced into the cell was determined volumetrically, that is, from the known volume of the cell (approximately 29.2 cm^3) and readings for temperature and pressure, using an appropriate equation of state, which was adopted from ref 10 for methane and from ref 11 for xenon, cf., the software package ThermoFluids.[12] The mass of the

* Corresponding author. E-mail: gmaurer@rhrk.uni-kl.de. Tel.: +49 631 205 2410. Fax: +49 631 205 3835.

10.1021/je700319x CCC: $37.00
Published on Web 09/08/2007

solvent (i.e., the ionic liquid [bmim][CH_3SO_4]) filled into the cell (about 34 g) was calculated from the volume displacement in a calibrated spindle press, which was used for the displacement of the solvent, and the solvent density.[1] The temperature was measured using two calibrated platinum resistance thermometers with an uncertainty of less than ± 0.1 K. When the cell was charged with methane (xenon), the pressure was recorded with two (three) pressure transducers suitable for a maximum pressure of 0.6 MPa and 1.6 MPa (0.6 MPa, 1.6 MPa, and 4 MPa). The corresponding solubility pressure was measured with three pressure transducers suitable up to 2.5 MPa, 10 MPa, and 25 MPa. All pressure transducers were purchased from WIKA GmbH, Klingenberg, Germany and calibrated against a high-precision pressure gauge (Desgranges and Huot, Aubervilliers, France) before and after each measurement series. The maximum systematic uncertainty in the solubility pressure measurement results from the intrinsic uncertainty of the pressure transducers (i.e., 0.1 % of the transducer's full scale) and an additional contribution of about ± 0.01 MPa from a small temperature drift inside the isolated (high-pressure) tubes filled with the solvent that connect the view-cell with the pressure transducers. Several test runs verified that particular drift.

Materials and Sample Pretreatment. Methane (4.5, mole fraction ≥ 0.99995) and xenon (4.0, mole fraction ≥ 0.9999) were purchased from Air Liquide Deutschland GmbH, Düsseldorf, Germany. Both gases were used without further purification. The ionic liquid [bmim][CH_3SO_4] ($C_9H_{18}N_2O_4S$, purum, mass fraction ≥ 0.98, dark yellow to brownish color, relative molar mass M = 250.32) was synthesized by Solvent Innovation GmbH, Cologne, Germany. The samples were degassed and dried under vacuum over a period of 2 days to remove traces of water and other volatile impurities. A glass burette served as sample container so that the ionic liquid could be handled and introduced into the apparatus under vacuum. The ionic liquid was collected after each measurement and reconditioned (i.e., degassed and dried under vacuum) for further use. No degradation was observed for [bmim][CH_3SO_4]. The multiple use led to an intensification of the color, but we could prove by repeating some experiments at conditions comparable to previously done measurements that this had no influence on the gas solubility. ^{1}H and ^{13}C NMR measurements were done both for the unprocessed ionic liquid and for a sample that had underwent treatment at 413 K. Both results proved to be equivalent. After completion of the measurement series, the water content of the sample was determined by Karl Fischer titration and found to be < 0.00099 mass fraction.

Experimental Results. Four isotherms of about (293, 333, 373, and 413) K were investigated up to approximately 10 MPa for both gases. The new solubility results are given in Tables 1 (for methane) and 2 (for xenon). The listed pressure p is the pressure required to dissolve a certain amount of the gas in one kilogram of the ionic liquid at a fixed temperature. The solubility pressure p is plotted versus the gas molality m_G (i.e., the amount of substance (the number of moles) of the gas per kilogram of [bmim][CH_3SO_4]) at constant temperature T in Figure 1 (left diagram for methane, right diagram for xenon).

Within the temperature and pressure regions investigated during this study, the solubility pressure monotonously increases with increasing gas molality at a given temperature. Figure 1 shows that the shape of the solubility isotherms is almost linear for methane. The solubility isotherms reveal purely physical solubility behavior for both methane and xenon, which is in accordance with prior investigations in [bmim][CH_3SO_4].[1,2] Methane is less soluble in [bmim][CH_3SO_4] than xenon, and the solubility decreases with increasing temperature for both gases, but this behavior is less pronounced for methane. For example, at p = 3 MPa about 0.079 (0.066) moles of methane {0.37 (0.18) moles of xenon} dissolve in one kilogram of [bmim][CH_3SO_4] at 293 K (413 K). The experiments showed that solution kinetics was slower for methane than for xenon, and higher temperatures accelerate the gas absorption. The state of equilibrium was accomplished after at a minimum of 2 (7) h for xenon (methane) at 293 K. At 413 K, that time span was lowered to 1 (2) h.

The experimental uncertainty for the gas molality Δm_G (caused by the filling procedure) was estimated from a Gauss

Table 1. Experimental Results for the Solubility of Gas G = Methane in [bmim][CH_3SO_4]

T / K	m_G / (mol·kg^{-1})	p / MPa	f_G/m_G / MPa/(mol·kg^{-1})
293.15 ± 0.1	0.03800 ± 0.00045	1.363 ± 0.035	35.0 ± 1.0
	0.06842 ± 0.00048	2.528 ± 0.036	35.3 ± 0.6
	0.10276 ± 0.00055	4.071 ± 0.039	36.8 ± 0.4
	0.13722 ± 0.00061	5.579 ± 0.041	36.8 ± 0.3
	0.17192 ± 0.00068	7.418 ± 0.044	37.8 ± 0.3
	0.19286 ± 0.00072	8.510 ± 0.045	38.0 ± 0.3
333.15 ± 0.1	0.04009 ± 0.00022	1.604 ± 0.028	39.3 ± 0.7
	0.07673 ± 0.00029	3.208 ± 0.031	40.4 ± 0.4
	0.10435 ± 0.00035	4.548 ± 0.034	41.5 ± 0.4
	0.13551 ± 0.00043	5.996 ± 0.037	41.5 ± 0.3
	0.15999 ± 0.00050	7.268 ± 0.040	42.1 ± 0.3
	0.18827 ± 0.00058	8.853 ± 0.043	42.9 ± 0.3
373.15 ± 0.1	0.03682 ± 0.00020	1.603 ± 0.028	43.1 ± 0.8
	0.05933 ± 0.00024	2.625 ± 0.030	43.5 ± 0.5
	0.08444 ± 0.00030	3.829 ± 0.033	44.2 ± 0.4
	0.11390 ± 0.00037	5.210 ± 0.036	44.3 ± 0.3
	0.14312 ± 0.00045	6.666 ± 0.039	44.7 ± 0.3
	0.17255 ± 0.00053	8.206 ± 0.043	45.3 ± 0.3
413.2 ± 0.1	0.03678 ± 0.00019	1.645 ± 0.028	44.5 ± 0.8
	0.06986 ± 0.00025	3.185 ± 0.031	45.1 ± 0.5
	0.10387 ± 0.00034	4.795 ± 0.035	45.4 ± 0.4
	0.13110 ± 0.00041	6.119 ± 0.038	45.7 ± 0.3
	0.15781 ± 0.00048	7.435 ± 0.041	46.0 ± 0.3
	0.18418 ± 0.00067	8.814 ± 0.050	46.5 ± 0.3

Table 2. Experimental Results for the Solubility of Gas G = Xenon in [bmim][CH_3SO_4]

T / K	m_G / (mol·kg^{-1})	p / MPa	f_G/m_G / MPa/(mol·kg^{-1})
293.1 ± 0.1	0.1553 ± 0.0008	1.194 ± 0.026	7.19 ± 0.17
	0.2327 ± 0.0011	1.840 ± 0.028	7.12 ± 0.13
	0.3122 ± 0.0013	2.525 ± 0.030	6.99 ± 0.10
	0.3855 ± 0.0016	3.158 ± 0.032	6.80 ± 0.09
333.15 ± 0.1	0.1302 ± 0.0007	1.417 ± 0.027	10.32 ± 0.22
	0.1904 ± 0.0009	2.116 ± 0.029	10.25 ± 0.16
	0.2589 ± 0.0011	2.939 ± 0.032	10.13 ± 0.13
	0.3829 ± 0.0016	4.534 ± 0.037	9.90 ± 0.11
	0.5010 ± 0.0020	6.298 ± 0.041	9.74 ± 0.10
	0.5896 ± 0.0027	8.030 ± 0.048	9.75 ± 0.10
	0.6520 ± 0.0029[a]	9.607 ± 0.050	9.78 ± 0.10
373.2 ± 0.1	0.1168 ± 0.0006	1.588 ± 0.028	13.04 ± 0.25
	0.2180 ± 0.0010	3.064 ± 0.033	12.95 ± 0.16
	0.2952 ± 0.0012	4.281 ± 0.036	12.92 ± 0.14
	0.3950 ± 0.0016	5.947 ± 0.041	12.81 ± 0.12
	0.4525 ± 0.0018	6.983 ± 0.044	12.75 ± 0.12
	0.5383 ± 0.0024	8.787 ± 0.052	12.81 ± 0.12
	0.6461 ± 0.0028	11.295 ± 0.072	12.78 ± 0.13
413.15 ± 0.1	0.1044 ± 0.0004	1.705 ± 0.019	15.81 ± 0.20
	0.1921 ± 0.0009	3.191 ± 0.034	15.63 ± 0.19
	0.2798 ± 0.0012	4.763 ± 0.039	15.54 ± 0.16
	0.3555 ± 0.0015	6.184 ± 0.043	15.46 ± 0.14
	0.4335 ± 0.0018	7.708 ± 0.048	15.35 ± 0.13
	0.5039 ± 0.0023[a]	9.280 ± 0.056	15.44 ± 0.14

[a] These experimental points were not taken into account for the extrapolation procedure to determine Henry's constant.

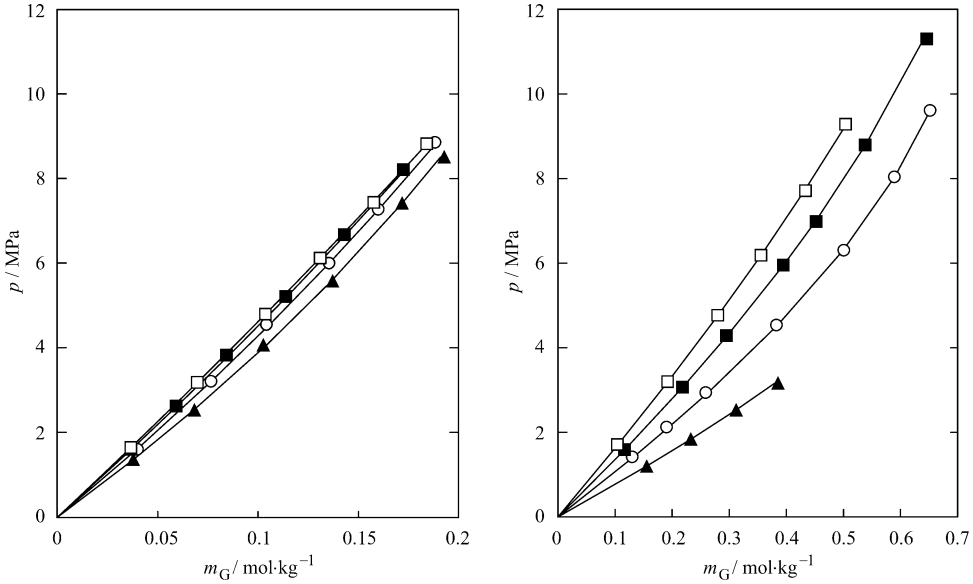

Figure 1. Total pressure above solutions of (gas G + [bmim][CH_3SO_4]): left diagram, G = CH_4; right diagram, G = Xe. ▲, ≈ 293 K; ○, ≈ 333 K; ■, ≈ 373 K; □, ≈ 413 K, experimental results; —, correlation.

error propagation calculation and amounts on average to 0.00043 mol·kg^{-1} (0.43 %) for the system methane + [bmim][CH_3SO_4] and to 0.00150 mol·kg^{-1} (0.44 %) for the system xenon + [bmim][CH_3SO_4]. The experimental uncertainty for the solubility pressure p was calculated from $\Delta p = \pm (\Delta p_{sys} + \Delta p_{stat})$. The first term accounts for the systematic uncertainties {i.e., pressure transducer's uncertainty (0.1 % of the transducer's full scale) + uncertainty resulting from the temperature drift (0.01 MPa)}. The second term is a statistical one from a Gauss error propagation calculation (by applying the vapor−liquid equilibrium (VLE) model described in the next section). It reflects the effect of the uncertainties of temperature and gas molality on the solubility pressure p. The absolute (relative) uncertainty in the pressure Δp ($\Delta p/p$) amounts on average to about 0.038 MPa (1 %) for both systems. The relative uncertainty decreases from (at maximum) 2.6 % at low pressures to (at minimum) 0.5 % at the highest pressure.

Correlation of the Gas Solubility

The correlation method applied here is congruent with that described in our previous work on the solubility of carbon dioxide.[1] Here, the approach is displayed for a better understanding. As usually accepted, a negligibly small vapor pressure is attributed to the ionic liquid [bmim][CH_3SO_4]. Consequently, the gaseous phase consists of the pure gas component, and the VLE condition is only applied to that gas component and results in the extended Henry's law:

$$k_{H,G}(T,p)a_G(T,m_G) = f_G(T,p) \quad (1)$$

$k_{H,G}(T,p)$ is Henry's constant of the gas (either methane or xenon) in [bmim][CH_3SO_4] at temperature T and pressure p (based on the molality scale). $a_G(T,m_G)$ is the activity of the gas in the liquid, and the influence of pressure on that activity is neglected. $f_G(T,p)$ is the corresponding fugacity in the vapor phase.

The Henry's constant of the gas in [bmim][CH_3SO_4] is expressed as

$$k_{H,G}(T,p) = k^{(0)}_{H,G}(T)\exp\left(\frac{V^{(\infty)}_{m,G}\,p}{RT}\right) \quad (2)$$

where $k^{(0)}_{H,G}(T)$ is the Henry's constant at zero pressure, $V^{(\infty)}_{m,G}$ is the partial molar volume of the gas at infinite dilution in the ionic liquid, and R is the universal gas constant.

The activity of the respective gas in the ionic liquid (on the molality scale) is

$$a_G = \frac{m_G}{m^\circ}\gamma_G \quad (3)$$

where $m^\circ = 1$ mol·kg^{-1}. The activity coefficient γ_G is calculated employing the virial expansion for the excess Gibbs energy (also on the molality scale) according to Pitzer:[13,14]

$$\ln \gamma_G = 2\frac{m_G}{m^\circ}\beta^{(0)}_{G,G} + 3\left(\frac{m_G}{m^\circ}\right)^2\mu_{G,G,G} \quad (4)$$

The parameters $\beta^{(0)}_{G,G}$ and $\mu_{G,G,G}$ describe binary as well as ternary interactions between gas molecules in the solvent.

Ultimately, the fugacity of the pure gas f_G at equilibrium temperature and pressure is the product of the total pressure p and the fugacity coefficient $\phi_G(T,p)$:

$$f_G(T,p) = p\phi_G(T,p) \quad (5)$$

The fugacity coefficients $\phi_G(T,p)$ were calculated with *ThermoFluids*.[12] An extrapolation (at fixed temperature) of the experimental results for the solubility pressure of the respective gas in [bmim][CH_3SO_4] gives Henry's constant of the gas in [bmim][CH_3SO_4] at zero pressure $k^{(0)}_{H,G}(T)$:

$$k^{(0)}_{H,G}(T) = \lim_{p\to 0}\left[\frac{f_G(T,p)}{(m_G/m^\circ)}\right] \quad (6)$$

The results for $f_G/(m_G/m^\circ)$ together with the estimated uncertainties are given in Tables 1 and 2 as well. Figure 2 shows the extrapolation to zero pressure for methane and xenon, respectively. Table 3 lists the numerical values for Henry's constant (at zero pressure and on the molality scale) after applying this procedure.

The estimated relative uncertainty for those Henry's constants amounts on average to 1.3 % for both methane and xenon. That

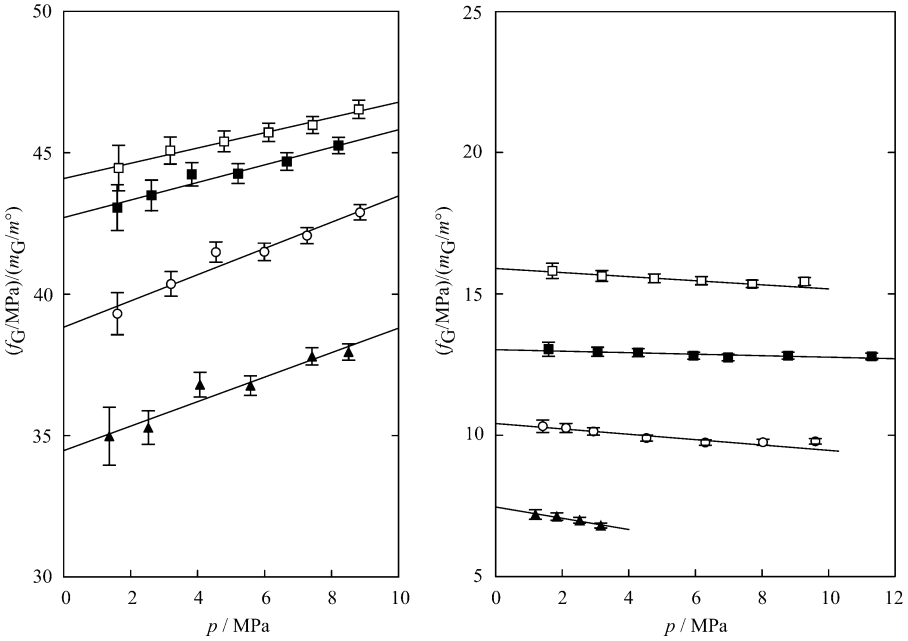

Figure 2. Influence of the total pressure on the ratio of the fugacity of gas G (in the gaseous phase) to the molality of that gas (in the ionic liquid [bmim][CH_3SO_4]): left diagram, G = CH_4; right diagram, G = Xe. ▲, ≈ 293 K; ○, ≈ 333 K; ■, ≈ 373 K; □, ≈ 413 K, experimental results (and estimated uncertainties); —, linear fit.

Table 3. Henry's Constant of the Gas G in [bmim][CH_3SO_4] (at Zero Pressure, on the Molality Scale)

gas G	T/K	$k^{(0)}_{H,G}$/MPa
methane CH_4	293.15	34.5 ± 0.5
	333.15	38.8 ± 0.5
	373.15	42.7 ± 0.5
	413.2	44.1 ± 0.5
xenon Xe	293.1	7.46 ± 0.13
	333.15	10.41 ± 0.12
	373.2	13.02 ± 0.14
	413.15	15.90 ± 0.16

uncertainty was estimated as follows: The number of experimental data points used in the extrapolation process should have no influence on the final result for Henry's constant as long as that number of experimental data points is sufficiently large. Therefore, the extrapolation was repeated omitting randomly selected single or double data points. The given uncertainty is the standard deviation between the optimum value (i.e., the result from all data points included) and the results from all these evaluations (i.e., with one or two data points omitted).

$$\ln(k^{(0)}_{H,CH_4}/\text{MPa}) = 6.216 - 564.5/(T/\text{K}) - 0.002566(T/\text{K}) \quad (7)$$

$$\ln(k^{(0)}_{H,Xe}/\text{MPa}) = 5.5906 - 928/(T/\text{K}) - 0.00141(T/\text{K}) \quad (8)$$

Equations 7 and 8 correlate the Henry's constant as a function of temperature. The deviation between experimental and correlated values for Henry's constant almost remains within the uncertainty that is given in Table 3. In Figure 3, both the data obtained from extrapolation to zero pressure and the correlation function for Henry's constant (cf. eqs 7 and 8) are plotted versus the inverse absolute temperature.

The results for the Henry's constant, that is to say, the correlation functions, the partial molar volume of either methane or xenon in [bmim][CH_3SO_4], $V^{(\infty)}_{m,G}$, and the expression for the Gibbs excess energy (on the molality scale) according to Pitzer (with interaction parameters $\beta^{(0)}_{G,G}$ and $\mu_{G,G,G}$), are the basis for

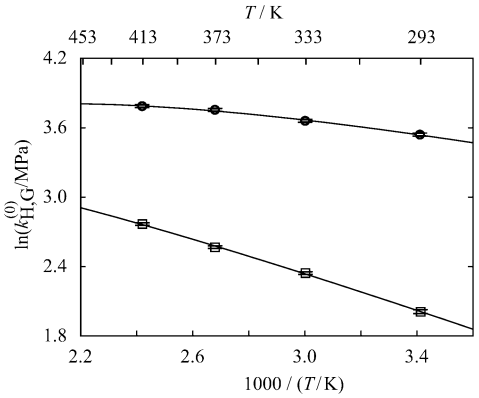

Figure 3. Henry's constant of gas G in [bmim][CH_3SO_4] (at zero pressure, on the molality scale) plotted against the (inverse) temperature: ○, G = CH_4; □, G = Xe, extrapolated experimental results (and estimated uncertainties); —, correlation.

the correlation of the solubility pressure. The curves in Figure 1 originate from this correlation.

For methane:

$$V^{(\infty)}_{m,CH_4}/(\text{cm}^3\cdot\text{mol}^{-1}) = 58.2 - 0.0931(T/\text{K}) \quad (9)$$

$$\beta^{(0)}_{CH_4,CH_4} = 0 \quad (10)$$

$$\mu_{CH_4,CH_4,CH_4} = 0 \quad (11)$$

For xenon:

$$V^{(\infty)}_{m,Xe}/(\text{cm}^3\cdot\text{mol}^{-1}) = -332.1 + 1.945(T/\text{K}) - 0.002513(T/\text{K})^2 \quad (12)$$

$$\beta^{(0)}_{Xe,Xe} = -0.1407 \quad (13)$$

$$\mu_{Xe,Xe,Xe} = 0 \quad (14)$$

The correlation results for the gas solubility (i.e., the gas molalities at a given temperature and solubility pressure) agree

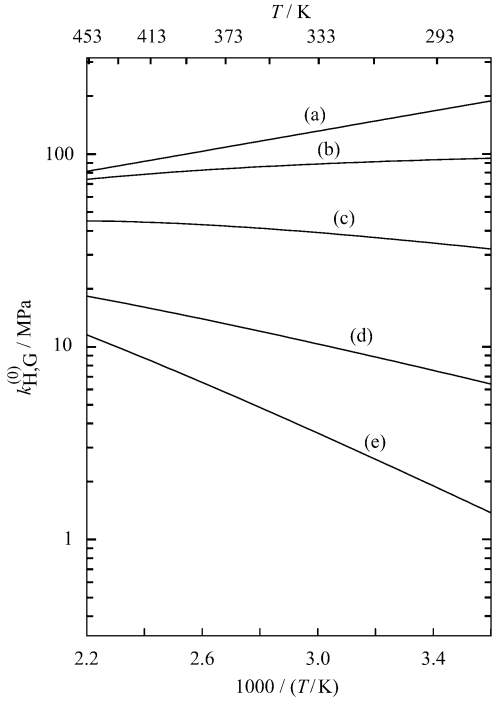

Figure 4. Correlation results for Henry's constant (at zero pressure, on the molality scale) of five different gases: (a) H_2, (b) CO, (c) CH_4, (d) Xe, and (e) CO_2 in [bmim][CH_3SO_4].

Table 4. Results for the Molar Solution Properties $\Delta_{sol}X_m$ at Standard Conditions (T° = 298.15 K, p° = 0.1 MPa) and on the Molality Scale from Henry's Constant

$\Delta_{sol}X^\circ_m$	methane	xenon
$\Delta_{sol}G^\circ_m$/(kJ·mol^{-1})	14.530 ± 0.032	10.811 ± 0.043
$\Delta_{sol}H^\circ_m$/(kJ·mol^{-1})	−2.8 ± 0.2	−6.7 ± 0.3
$\Delta_{sol}S^\circ_m$/(J·mol^{-1}·K^{-1})	−58.1 ± 0.5	−58.7 ± 0.9
$\Delta_{sol}C^\circ_{p,m}$/(J·mol^{-1}·K^{-1})	12.7 ± 0.3	7.1 ± 1.6

with the data from the laboratory experiment within an average absolute (relative) deviation of about 0.00053 mol·kg^{-1} (0.5 %) for the system methane + [bmim][CH_3SO_4] and of about 0.0015 mol·kg^{-1} (0.5 %) for the system xenon + [bmim][CH_3SO_4].

Knowing Henry's constant enables the calculation of various related (molar) solution thermodynamic properties, $\Delta_{sol}X_m$, where, for example, X can be replaced by G (i.e., the Gibbs energy), H (i.e., the enthalpy), S (i.e., the entropy), or C_p (i.e., the heat capacity at constant pressure).[15] Table 4 shows the resulting values at standard conditions (T° = 298.15 K, p° = 0.1 MPa) and on the molality scale that result from the correlation equations given above. The molar solution properties at standard conditions of both investigated gases are of similar magnitude as those for the previously investigated gases (carbon dioxide (cf. Kumełan et al.[1]), carbon monoxide and hydrogen (cf. Kumełan et al.[2]).

Discussion

To illustrate the different solubility behavior of the gases that were investigated by us so far, Henry's constants for all these gases in [bmim][CH_3SO_4] (at zero pressure and on the molality scale) are plotted versus the inverse temperature in Figure 4. The curves give correlation results only from our own experiments.

First, the sequence of these curves indicates that, at least within the investigated temperature range, carbon dioxide has the largest solubility, followed by xenon, methane, carbon monoxide, and ultimately hydrogen. Second, the slope of these curves displays a decreasing gas solubility with increasing temperature for carbon dioxide, xenon, and methane, diminishing within this sequence, but a reversely increasing gas solubility with rising temperature for carbon monoxide and hydrogen. A similar gas solubility trend was observed in [bmim][PF_6].[1,15,18−20] It is well known from the literature[16,17] that the illustrated curves converge at the critical temperature of the solvent. At that point, the slope of all those curves is equal to infinity. However, because ionic liquids decompose at high temperatures, it may not be possible to determine their critical temperature.

In a concluding statement, our experiments identified an ionic liquid as a solvent with the capability to absorb significant amounts of xenon already at relatively moderate conditions. We might assume that other ionic liquids behave similarly.

Referring to the aforementioned example of clinical xenon administration,[8] 16 L of gaseous xenon (at 293.15 K and 0.101325 MPa) correspond to about 87.8 g or 0.67 mol xenon.[10] Our solubility experiments show that, for example, about 2.5 kg of [bmim][CH_3SO_4] could absorb that amount of xenon at 333 K under a pressure of 3 MPa or about 1 kg at the same temperature but at 9 MPa. In principle, these particular characteristics could perhaps be considered in design of a recycling process.

Conclusions

To our knowledge for the first time ever, we report experimental results for the solubility of the single gases methane and xenon in the ionic liquid [bmim][CH_3SO_4] from about 293 K to 413 K and up to approximately 10 MPa. By using the solubility data, Henry's law constants were determined and solution thermodynamic properties for these two binary systems were calculated. The gas solubility (i.e., the gas molality at given temperature and pressure) was correlated by an extension of Henry's law with an average relative deviation of about 0.5 % for both systems methane + [bmim][CH_3SO_4] and xenon + [bmim][CH_3SO_4].

Acknowledgment

The authors thank Dr. K. Massonne, BASF Aktiengesellschaft, Ludwigshafen, Germany, for generously supplying the ionic liquid [bmim][CH_3SO_4].

Literature Cited

(1) Kumełan, J.; Pérez-Salado Kamps, Á.; Tuma, D.; Maurer, G. Solubility of CO_2 in the ionic liquids [bmim][CH_3SO_4] and [bmim][PF_6]. *J. Chem. Eng. Data* **2006**, *51*, 1802−1807.

(2) Kumełan, J.; Pérez-Salado Kamps, Á.; Tuma, D.; Maurer, G. Solubility of the single gases H_2 and CO in the ionic liquid [bmim][CH_3SO_4]. *Fluid Phase Equilib.* **2007**, *260*, 3−8.

(3) Anthony, J. L.; Maginn, E. J.; Brennecke, J. F. Solubilities and thermodynamic properties of gases in the ionic liquid 1-*n*-butyl-3-methylimidazolium hexafluorophosphate. *J. Phys. Chem. B* **2002**, *106*, 7315−7320.

(4) Anthony, J. L.; Crosthwaite, J. M.; Hert, D. G.; Aki, S. N. V. K.; Maginn, E. J.; Brennecke, J. F. Phase equilibria of gases and liquids with 1-*n*-butyl-3-methylimidazolium tetrafluoroborate. In *Ionic Liquids as Green Solvents. Progress and Prospects*; Rogers, R. D., Seddon, K. R., Eds.; ACS Symposium Series 856; American Chemical Society: Washington, DC, 2003; pp 110−120.

(5) Lynch, C., III; Baum, J.; Tenbrinck, R. Xenon anesthesia. *Anesthesiology* **2000**, *92*, 865−868.

(6) Marx, T.; Schmidt, M.; Schirmer, U.; Reinelt, H. Xenon anaesthesia. *J. R. Soc. Med.* **2000**, *93*, 513−517.

(7) Reyle-Hahn, M.; Rossaint, R. Xenon − A new anaesthetic gas. *Anaesthesist* **2000**, *49*, 869−874.

(8) Goto, T.; Nakata, Y.; Morita, S. Will xenon be a stranger or a friend? The cost, benefit, and future of xenon anesthesia. *Anesthesiology* **2003**, *98*, 1−2.

(9) Leclerc, J.; Nieuviarts, R.; Tavernier, B.; Vallet, B.; Scherpereel, P. Xenon anaesthesia: from myth to reality. *Ann. Fr. Anesth. Réanim.* **2000**, *20*, 70−76.
(10) Setzmann, U.; Wagner, W. A new equation of state and tables of the thermodynamic properties for methane covering the range from the melting line to 625 K at pressures up to 1000 MPa. *J. Phys. Chem. Ref. Data* **1991**, *20*, 1061−1155.
(11) Lemmon, E. W.; Span, R. Short fundamental equations of state for 20 industrial fluids. *J. Chem. Eng. Data* **2006**, *51*, 785−850.
(12) Wagner, W.; Overhoff, U. *ThermoFluids*, Version 1.0 (Build 1.0.0). Springer: Berlin, 2006.
(13) Pitzer, K. S. Thermodynamics of electrolytes. 1. Theoretical basis and general equations. *J. Phys. Chem.* **1973**, *77*, 268−277.
(14) Pitzer, K. S. Ion Interaction Approach: Theory and Data Correlation. In *Activity Coefficients in Electrolyte Solutions*; Pitzer, K. S., Ed.; CRC Press: Boca Raton, FL, 1991; pp 75−155.
(15) Pérez-Salado Kamps, Á.; Tuma, D.; Xia, J.; Maurer, G. Solubility of CO_2 in the ionic liquid [bmim][PF_6]. *J. Chem. Eng. Data* **2003**, *48*, 746−749.
(16) Beutier, D.; Renon, H. Gas solubilities near the solvent critical point. *AIChE J.* **1978**, *24*, 1122−1125.
(17) Schotte, W. Solubilities near the solvent critical point. *AIChE J.* **1985**, *31*, 154−157.
(18) Kumełan, J.; Pérez-Salado Kamps, Á.; Urukova, I.; Tuma, D.; Maurer, G. Solubility of oxygen in the ionic liquid [bmim][PF_6]: Experimental and molecular simulation results. *J. Chem. Thermodyn.* **2005**, *37*, 595−602; **2007**, *39*, 335.
(19) Kumełan, J.; Pérez-Salado Kamps, Á.; Tuma, D.; Maurer, G. Solubility of CO in the ionic liquid [bmim][PF_6]. *Fluid Phase Equilib.* **2005**, *228*−*229*, 207−211.
(20) Kumełan, J.; Pérez-Salado Kamps, Á.; Tuma, D.; Maurer, G. Solubility of H_2 in the ionic liquid [bmim][PF_6]. *J. Chem. Eng. Data* **2006**, *51*, 11−14.

Received for review June 5, 2007. Accepted July 30, 2007. The authors appreciate financial support by Deutsche Forschungsgemeinschaft (DFG), Bonn-Bad Godesberg, Germany.

JE700319X